Chasing cosmic tau neutrinos in the abyss

Bormuth, R.; Bormuth R.

Citation

Bormuth, R. (2017, December 7). *Chasing cosmic tau neutrinos in the abyss*. *Casimir PhD Series*. Retrieved from https://hdl.handle.net/1887/56023

Cover Page

Universiteit Leiden

Leiden University
Repository

The handle http://hdl.handle.net/1887/56023 holds various files of this Leiden University dissertation.

Author: Bormuth, R.
Title: Chasing cosmic tau neutrinos in the abyss
Issue Date: 2017-12-07

TAU "DOUBLE BANG" SELECTION

And I heard, as it were, the noise
of thunder
One of the four beasts saying,
'Come and see.' and I saw, and
behold a white horse

Johnny Cash, The Man Comes
Around

In this chapter the selection criteria to identify "Double Bang" events using the Belle Starr reconstruction are presented. The assumed neutrino flux corresponds to the measured flux of high energy neutrinos by IceCube (see Sec. 1.2.5). The optimization of the selection criteria is performed using an energy spectrum of $E^{2.46}$ (see Chap. 5) with a 3 PeV cut-off. This spectrum is in accordance with the best fit to the IceCube data of $\Gamma = 2.5 \pm 0.9$ [121]. The reason for choosing $\Gamma = 2.46$ instead of $\Gamma = 2.5$ is the compatibility with the considered spectra in the KM3NeT LoI [67]. The spectral index has a large impact on the amount of reconstructable "Double Bang" events, since the tau travel length and therefore the separation between the two showers, depends on the tau energy.

In this chapter, the considered background channels are the neutrino interactions numuCC, nueCC, NC and atmospheric muons. In the last section, the influence of atmospheric neutrinos on the final results is presented.

For the atmospheric muons the MC simulation with a minimum leading muon energy of 50 TeV (threshold at the can) is used. The reason being, that high energy muons are more likely to mimic "Double Bang" events and lower threshold simulations do not offer sufficient statistics at high energies. Only neutrino events are considered, since at energies exceeding 10 TeV no significant differences between neutrinos and anti-neutrinos is expected.

6.1 SELECTION CRITERIA

So far, a first basic set of selection criteria was developed without performing a full optimization. The selection criteria are chosen to achieve a large signal yield and little remaining background with special attention to reducing the atmospheric muons background as much as possible.

With regard to these goals, five selection variables have been identified which show good discriminating power between signal and background signatures, namely: the logarithm of the reconstructed energy (energy cut), the position of the reconstructed vertices relative to the detector (position cut), the number of peaks in the likelihood scan (peak cut), the probability of hits to be optical
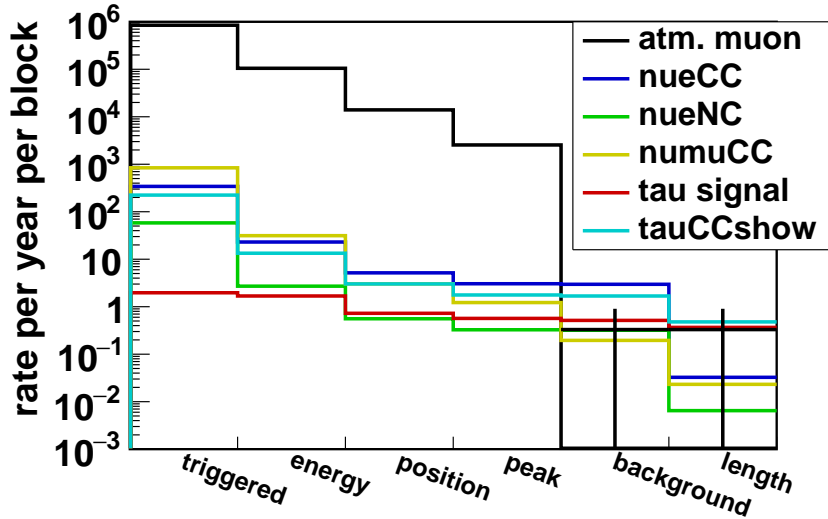
Figure 80: Inclusive event rates per block and year for different channels after applying the selection criteria.

background (background cut) and the reconstructed tau flight length (length cut). The values for the different cuts are chosen as follows:

- energy cut: $E_{rec} \geqslant 10^{4.5} \, \text{GeV}$

- position cut:
    - Prefit position $Z \leqslant 250 \, \text{m}$ and exclusion of outer part of detector
    - Refit positions $-300 \, \text{m} \leqslant Z \leqslant 250 \, \text{m}$ and $R_{xy} \leqslant 390 \, \text{m}$

- peak cut: $n_{peaks} = 1, 2$

- background cut: $P(bkg) \geqslant 10^{-6}$

- length cut: reconstructed length $\geqslant 5 \, \text{m}$

Applying these selection cuts to the MC simulations results in the distribution shown in Fig. 80. The X-axis shows the applied cuts from left to right and the Y-axis shows the inclusive rate for the different channels. Since the background cut rejects all simulated atmospheric muons the last two bins of the muon distribution show an estimation of the rejection performance based on the lifetime of the simulation. The lifetime, for the used atmospheric muon simulation, is 0.33 events per year per block for a single event. Therefore, the bin values after previous cuts are applied is set to the weight of a single event and the errors are set to the corresponding Poisson probability.

The order in which the cuts are applied to the events was chosen such that variables which reject the same background signatures are grouped together, resulting in the trend shown in Fig. 80: The energy cut rejects all background channels equally, the position, peaks and background cuts reject mainly track like channels and the length cut rejects mainly single shower like channels.

In the following, the different selection variables will be explained and their efficiencies discussed in detail. For all but the position cut, their distribution is shown three times for different selections: the distribution of all triggered events, the distribution after application of the previous steps and the distribution after all other cuts have been applied. The first distribution allows for a general characterization of the variable under investigation, the second shows the distribution of events that are subject to the current selection and the third indicates the effectiveness of the current selection. For the third histogram also a cumulative distribution is shown. Since the position cut involves two dimensions, the distributions will be separately shown.

6.1.1 *Energy cut*

"Double Bang" events can effectively be distinguished from single shower events if the tau lepton travels visible distances before its decay. As discussed in more detail in Sec. 5.1, the tau travels visible distances at energies around $\mathcal{O}(100\,\text{TeV})$ and higher (or $\log(E\,[\text{GeV}]) = 5$). Therefore, a selection based on the reconstructed energy is a natural choice given the "Double Bang" kinematics and the large population of background events at lower energies.

The distribution of the reconstructed energy of all channels is shown in Fig. 81a. The dependence of the tau flight length on the energy is visible for the tau signal channel. The rate of tau signal events decreases for reconstructed energies below $\log(E_{\text{rec}}\,[\text{GeV}]) = 5$. Above this energy, the tau signal events follow the tauCCshow curve up to $\log(E_{\text{rec}}\,[\text{GeV}]) = 6$. The latter deviation is caused by the tau flight length becoming so large, that the containment criterion for tau signal events rejects these events. The three neutrino channels show the expected behavior assuming an energy spectrum following a power law with $\gamma = -2.46$. The structure in the distribution of the reconstructed energy of the atmospheric muons is a feature of the simulation in which an energy threshold of $50\,\text{TeV}$ (which corresponds to $\log(E\,[\text{GeV}]) = 4.7$) is applied. Most of these muons deposit significantly less energy in the detector.

The distribution of the reconstructed energies after all the other selection criteria is shown in Fig. 81c. Here, a cut-off is present in both tau signal and tauCCshow channels at reconstructed energies of $\log(E_{\text{rec}}\,[\text{GeV}]) = 4.5$. The reason for the cut-off edge to be so pronounced is the Bjorken y distribution. Whilst there are events with tau flight lengths longer than $5\,\text{m}$ at energies below the cut-off, the Bjorken y values must then be very close to one. This makes a successful reconstruction of these events very unlikely. The populations of atmospheric muons at low energies are typically caused by events with a very asymmetric distributions of hits in the detector.

As can be seen from Fig. 81d, the final selection on the reconstructed energy of $\log(E_{\text{rec}}\,[\text{GeV}]) \geqslant 4.5$ rejects all atmospheric muons and about $50\,\%$ of the neutrino background channels while keeping almost all signal events.

(a) Reconstructed energy after triggering.

(b) Reconstructed energy in selection variable sequence (same as Fig. 81a).

(c) Reconstructed energy after all other cuts applied.

(d) Cumulative distribution of Fig. 81c; Magenta line indicates cut value.

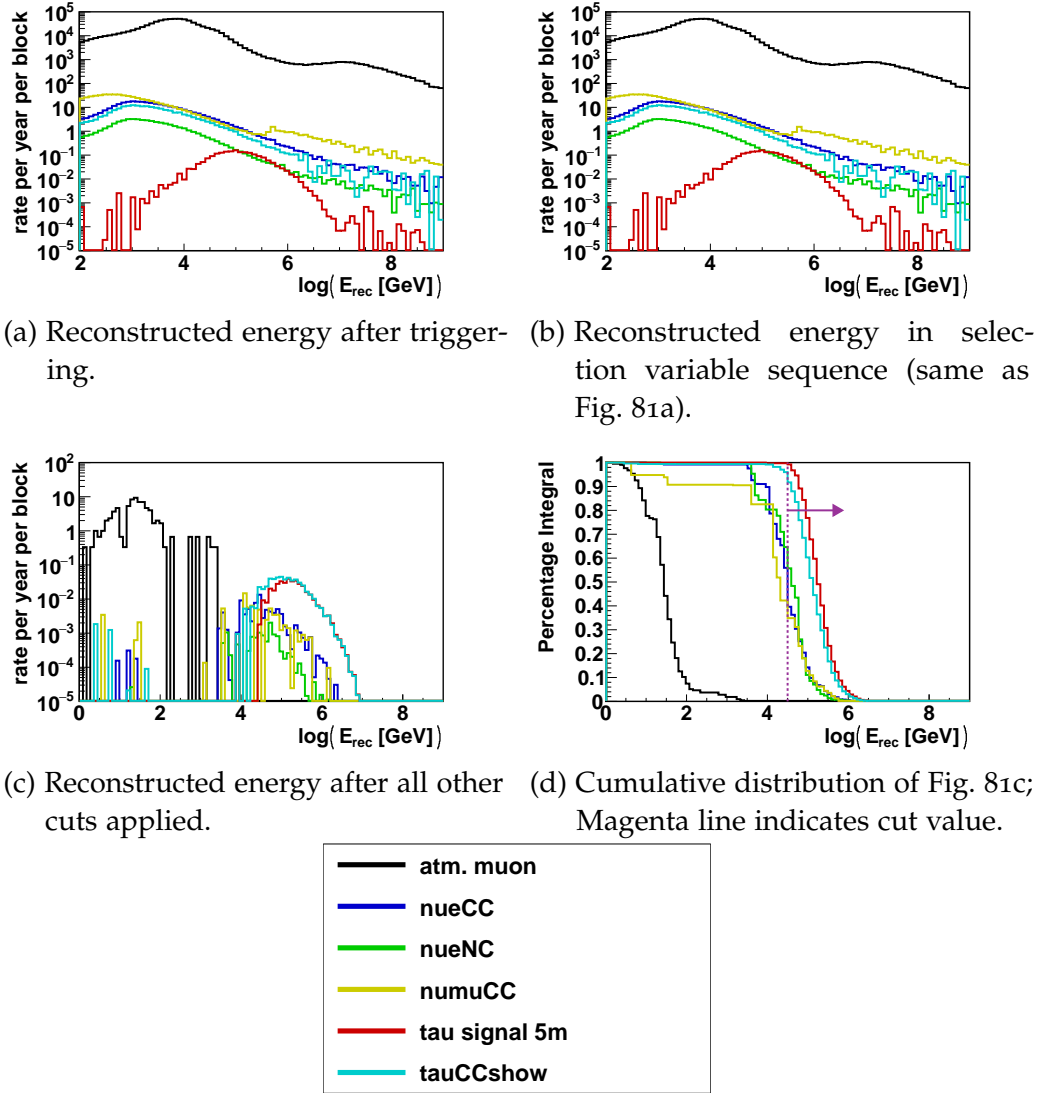|	
———	atm. muon
———	nueCC
———	nueNC
———	numuCC
———	tau signal 5m
———	tauCCshow

Figure 81: Distribution of the reconstructed energies for the different channels.

6.1.2 *Position cut*

The containment of the reconstructed vertices is crucial to support a good reconstruction performance. Additionally, the Position cut will help to suppress the atmospheric muon background. Reason being, that the characteristic zenith angle distribution of atmospheric muons yields reconstructed vertices at the sides and top of the detector. Whereas neutrinos arrive at the detector from all directions apart from a small bias for downward directions due to the possible absorption in the Earth.

For an early rejection of atmospheric muons, the position cut is applied to the reconstructed Prefit position. Note that for the Prefit early hits are selected, thereby biasing the Prefit vertex towards positions at the start of a track. Thereby causing the vertex for atmospheric muons to be pushed upstream the muon trajectory towards the outside of the detector volume, while for neutrinos the vertex is pushed towards theiro interaction points.

The reconstructed Prefit positions for atmospheric muons and tauCCshow events are shown in Fig. 82a and Fig. 82b, respectively. The atmospheric muons are indeed biased towards the top and outer edge of the detector while the tauCCshow events show no such bias. The visible pattern is caused by the regular DOM positions. The Prefit is known to prefer positions close to a set of DOMs.

The same position bias is observed for both channels after the other selection criteria are applied as shown in Fig. 82c and Fig. 82d. As can be seen, most of the remaining atmospheric muons events have a reconstructed vertex position within the top 50 m of the detector volume. A top view of these events is shown in Fig. 82e. Comparing the positions to the detector top view in Fig. 82f, it is clear that most of the events are located between the two outer layers of the detector. Applying a selection which rejects that volume as indicated by the red line in Fig. 82f therefore rejects most of the atmospheric muon events.

The remaining atmospheric muons are rejected by requiring the positions of the two reconstructed vertices after the Refit to be contained within the detector. This selection also works well for "Double Bang" events, as edge effects are avoided and reconstructed positions outside the detector volume most likely yield bad reconstruction performances.

In summary, two different positions are utilized for the position cut: the Prefit and the final vertex positions. For the Prefit position, the height is required to be lower than 250 m and the radial distance from the detector center is required to be within the inner part shown in Fig. 82f. For the Refit positions the height is also required to be less than 250 m and the radius to be less than 400 m.

6.1.3 *Peak cut*

The number of significant peaks found in the likelihood scan by Belle Starr Peak constitutes a selection variable which is ideally suited for suppressing track signatures. The reason being, that every Bremsstrahlungs shower along the track with a sufficient number of hits will produce a peak. Therefore, the likelihood scan is expected to have a varying number of significant peaks for track events, one significant peak for contained single shower events and one or two significant peaks for contained "Double Bang" events. This feature can be seen in Fig. 83a. While the tau signal channel shows similar number of events with zero, one or two significant peaks, the other channels show a large contribution of events with zero or more than two significant peaks. Especially the track channels show tails towards large numbers of significant peaks.

The same distribution after the energy and position cuts have been applied is shown in Fig. 83b. While the distribution of events did not change much, the nueCC and tauCCshow distribution now show a maximum at one significant peak and the tau signal distribution shows mainly one or two significant peaks.
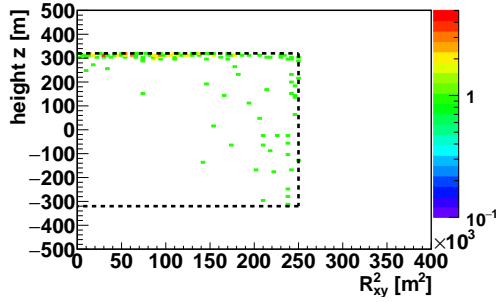
With all other cuts applied, the remaining atmospheric muon events have zero significant peaks and the numuCC events have a small tail with more than two significant peaks as can be seen from Fig. 83c. Therefore, the accepted
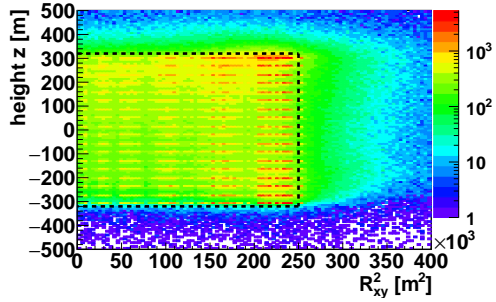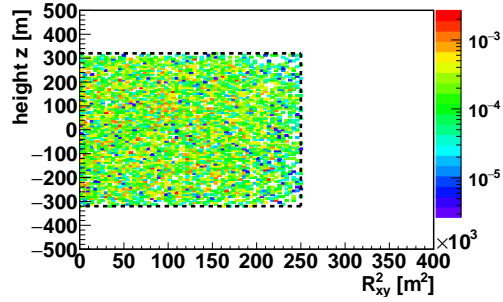
(a) Positions of atmospheric muon trig-
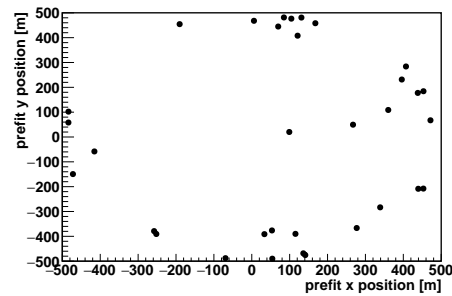gered events.
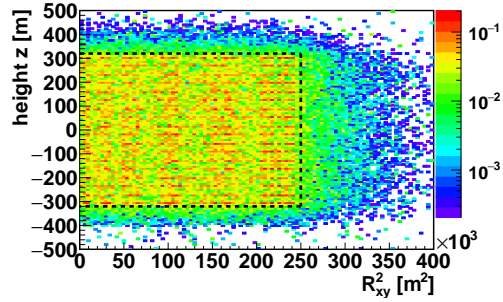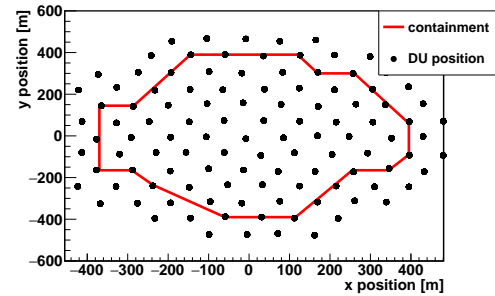
(b) Positions of tauCCshow triggered
events.

(c) Positions of atmospheric muons
events after other selection criteria.

(d) Positions of tauCCshow events after
other selection criteria.

(e) Top view of the detector for atmo-
spheric muons with $z \leqslant 250\,\text{m}$.

(f) DU position in top view; red line
marks inner part.

Figure 82: Distributions of reconstructed Prefit vertex positions in the instru-
mented volume for atmospheric muon and "Double Bang" events;
in the top 4 plots the black dotted line indicates the detector volume.

(a) Number of peaks after triggering.

(b) Number of peaks after energy and position cuts.

(c) Number of peaks after all other cuts are applied.

(d) Cumulative distribution of Fig. 83c; Events between the magenta lines are selected.

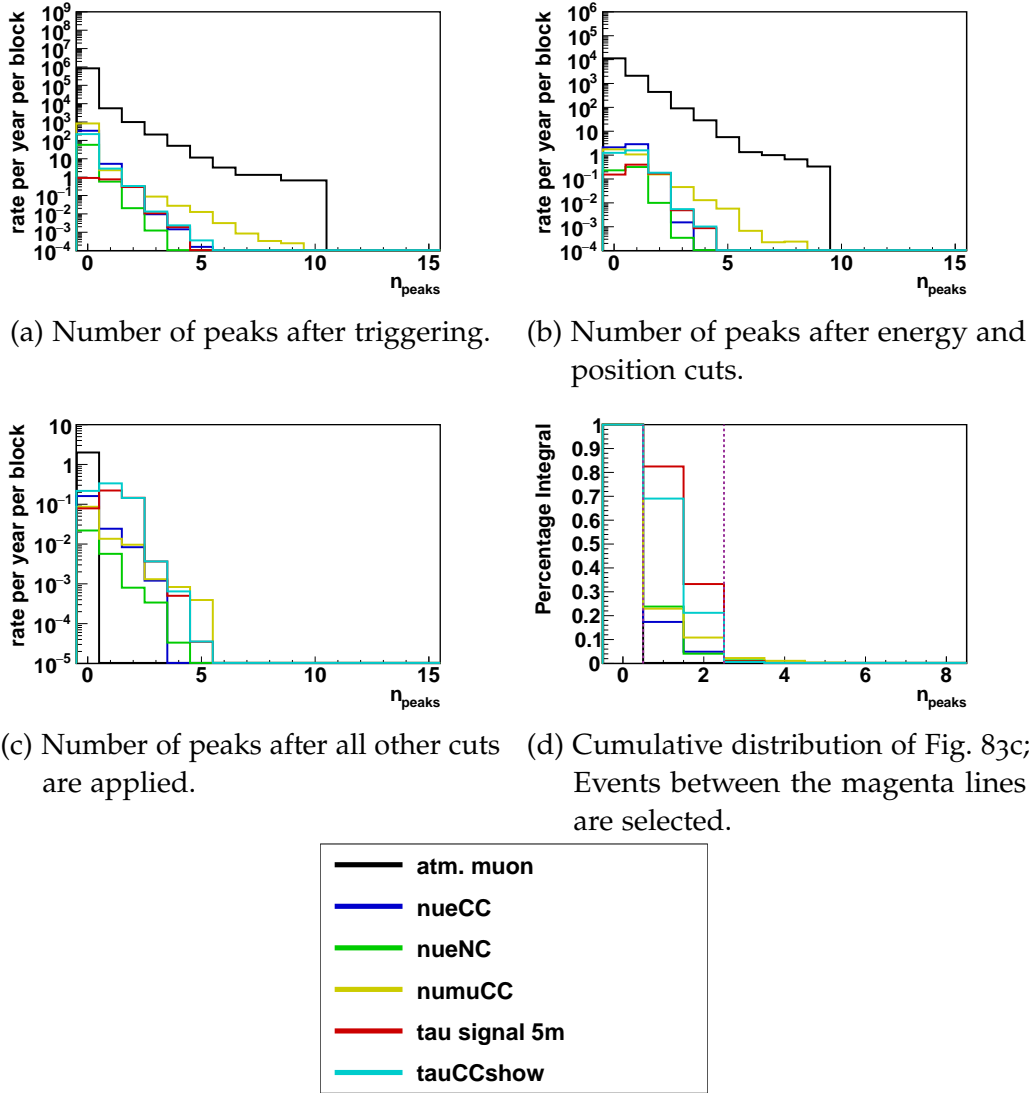|	atm. muon
	nueCC
	nueNC
	numuCC
	tau signal 5m
	tauCCshow

Figure 83: Distributions of the number of peaks for different channels.

number of significant peaks is set to be one or two. As can be seen from Fig. 83d, this cut rejects all remaining atmospheric muon events while keeping 82 % of the signal events.

6.1.4 *Background cut*

The background cut is a criterion to distinguish track events from "Double Bang" events. It uses the fact that track events contain a substantial number of photons which do not originate from either of the reconstructed shower positions. This is not the case for "Double Bang" events, because the tau lepton is minimal ionizing and the tau flight length is much shorter than that of muons at energies of interest. Therefore, the hits which cannot originate from either reconstructed vertex are caused by a signature different from "Double Bangs" or are optical background.
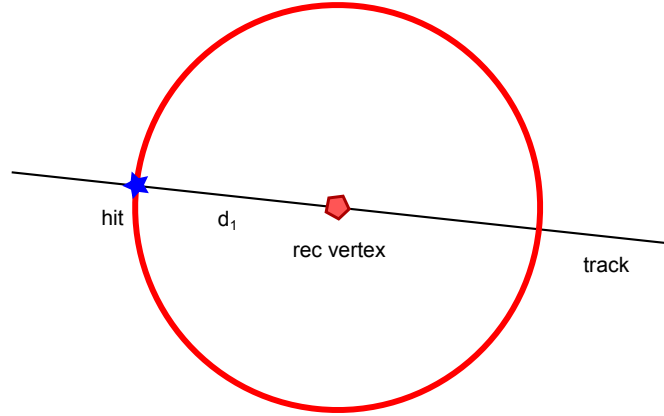
Figure 84: Estimated earliest hit time residual for chosen radius d_1 with respect to the reconstructed vertex.

In order to select the hits which cannot originate from either shower, the hit time residuals as defined in Eq. 24 are used. As can be seen from Fig. 66, the hit time residual distribution for showers at different energies has a long tail towards positive residuals and a sharp edge for negative residuals, with almost no hit time residuals below -20 ns. Because of this strict cut-off, selecting hits with hit time residuals $\Delta T \leqslant -20$ ns with respect to both reconstructed vertices will select hits not originating from either reconstructed vertex. Only hits within a certain radius around both the reconstructed vertex positions are considered. By limiting the radius, the total number of hits is dramatically reduced while only a small fraction of hits from any signature are lost in the process.

A suitable radius around the reconstructed vertices was found to be $d_1 = 200$ m. The choice of the considered radius translates to a lower limit for the hit time residuals. The lowest possible hit time residual is that of a track event if a hit is emitted from the track at exactly $d_1 = 200$ m distance to one of the reconstructed vertices. The reason being, that the muon travels faster than the light in the actual medium. The hit time residual of a hit which is emitted and detected at exactly d_1 distance to a reconstructed vertex is given by the travel time of the of the muon to the reconstructed vertex and the light travel time back to the hit position as shown in Fig. 84. This causes a minimal negative time residual as given by Eq. 34 of $\Delta T_{min} = -1588$ ns for $d_1 = 200$ m. In order to avoid edge effects the value is increased to $\Delta T_{min} = -1600$ ns.

$$\Delta T_{min} = -1 \times (d_1/c + d_1/c_{water}) \quad . \tag{34}$$

To summarize, the selection is composed of a cut on the distance of the hits to either reconstructed vertex to be smaller than 200 m and a cut on the hit time residuals towards both reconstructed shower vertices to be $\Delta T_{min} = -1600$ ns $\leqslant \Delta T \leqslant \Delta T_{max} = -20$ ns.

For this hit selection, the expected number of optical background hits is given by:

$$N_{bkg} = N_{PMT} \times (\Delta T_{min} - \Delta T_{max}) \times R_{bkg} \quad , \tag{35}$$

where N^{PMT} is the number of PMTs present in the considered volume and R_{bkg} is the expected optical background rate. For the background rate a value of $5\,kHz$ is used which corresponds to the background rate observed with the string prototype (see Chap. 4). For this single rate and an average of 2100 PMTs for the considered volume, the expected number of optical background hits is $N_{bkg} = 16.6$. This number will vary from event to event as the PMTs are not distributed evenly in the detector.

For an event the number of selected hits is then compared to the number of expected background hits. This is done using the Poisson probability of the selected hits being background, P(bkg), the distribution of the logarithm of P(bkg) can be seen from Fig. 85. As shown in Fig. 85a for all triggered events and channels the distribution is peaked around -3.5 with a tail towards smaller values. The peak at -3.5 is caused by low energy events which produce a small number of hits in the detector which is not significant compared to the random background hypothesis.

As can be seen from Fig. 85b, the distributions change after the previous selections. The distribution of the shower channels are peaked at log P(bkg)=-2 while the numuCC channel has large tails with an offset of -10 from zero. After all other cuts are applied the numuCC channel is essentially flat, while the distribution of the muon channel remains unchanged as can be seen from Fig. 85c. The cumulative distribution of log P(bkg) after other selection variables is shown in Fig. 85d. A cut of P(bkg)$\geqslant 10^{-6}$ is defined which selects more than 95 % of the "Double Bang" signal while rejecting the remaining atmospheric muon events and 90 % of the remaining numuCC events.

6.1.5 *Length cut*

The length cut is a criterion to distinguish single shower events from "Double Bang" events, since for well reconstructed single shower events both reconstructed vertices are expected to be at the same position. Therefore, selecting a minimum reconstructed length between the two vertices rejects single shower events.

The distributions of the reconstructed lengths can be seen in Fig. 86. Since the Belle Starr Refit algorithm is only run for a sub sample of events, the reconstructed length for all triggered events is combination of results from either the Scan, Peak or Refit module. This causes the plateau at lengths greater than $200\,m$.

This behavior changes when the other selection variables are applied as can be seen from Fig. 86b and Fig. 86c which are identical since the length cut is the last cut to be applied. The distributions of single shower and track events peak at reconstructed lengths smaller than $5\,m$ with the track events having some
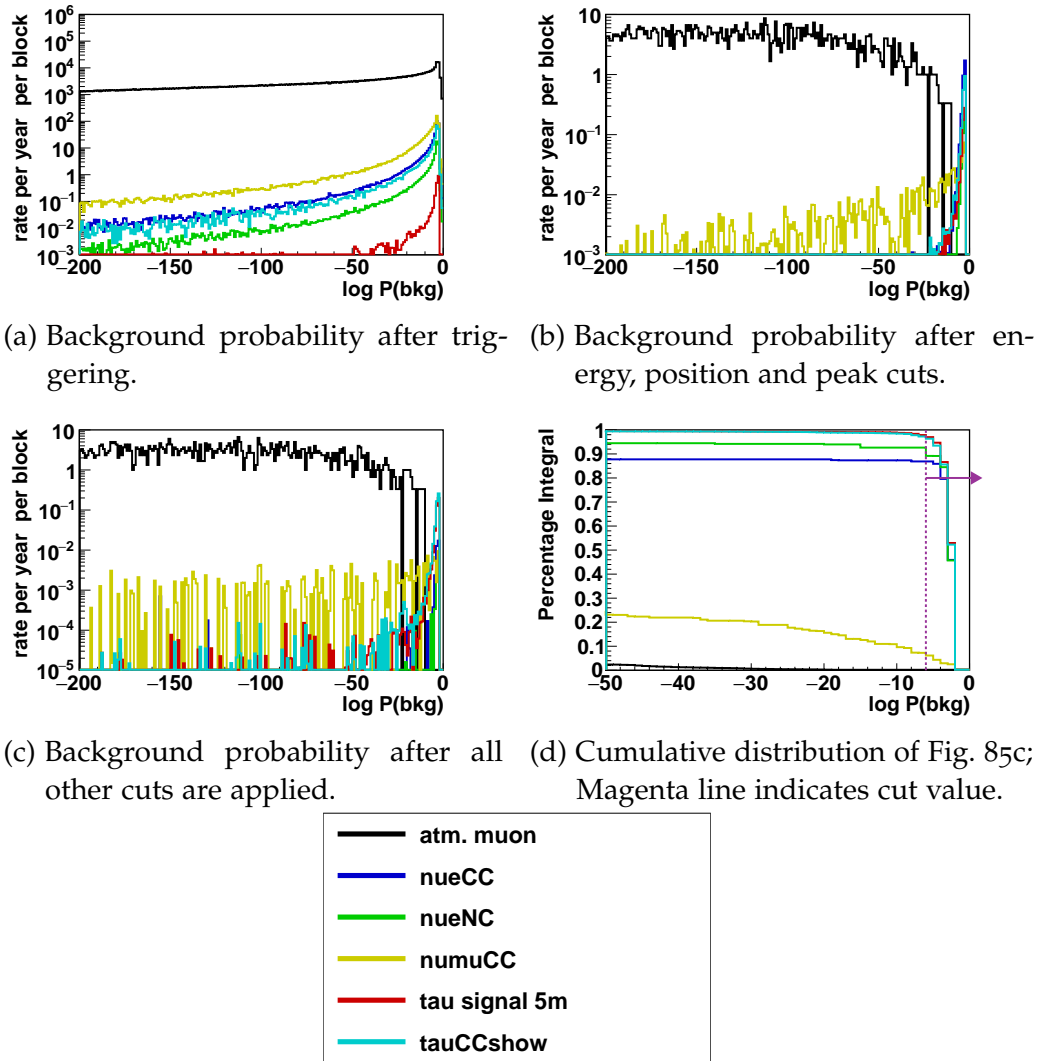
(a) Background probability after triggering.

(b) Background probability after energy, position and peak cuts.

(c) Background probability after all other cuts are applied.

(d) Cumulative distribution of Fig. 85c; Magenta line indicates cut value.

——	atm. muon
——	nueCC
——	nueNC
——	numuCC
——	tau signal 5m
——	tauCCshow

Figure 85: Distributions of the background probabilities for the different channels.

(a) Reconstructed length after trigger-
ing.

(b) Reconstructed length after energy,
position, peak and background
cuts.

(c) Reconstructed length after all other
cuts are applied.

(d) Cumulative distribution of Fig. 86c;
Magenta line indicates cut value.

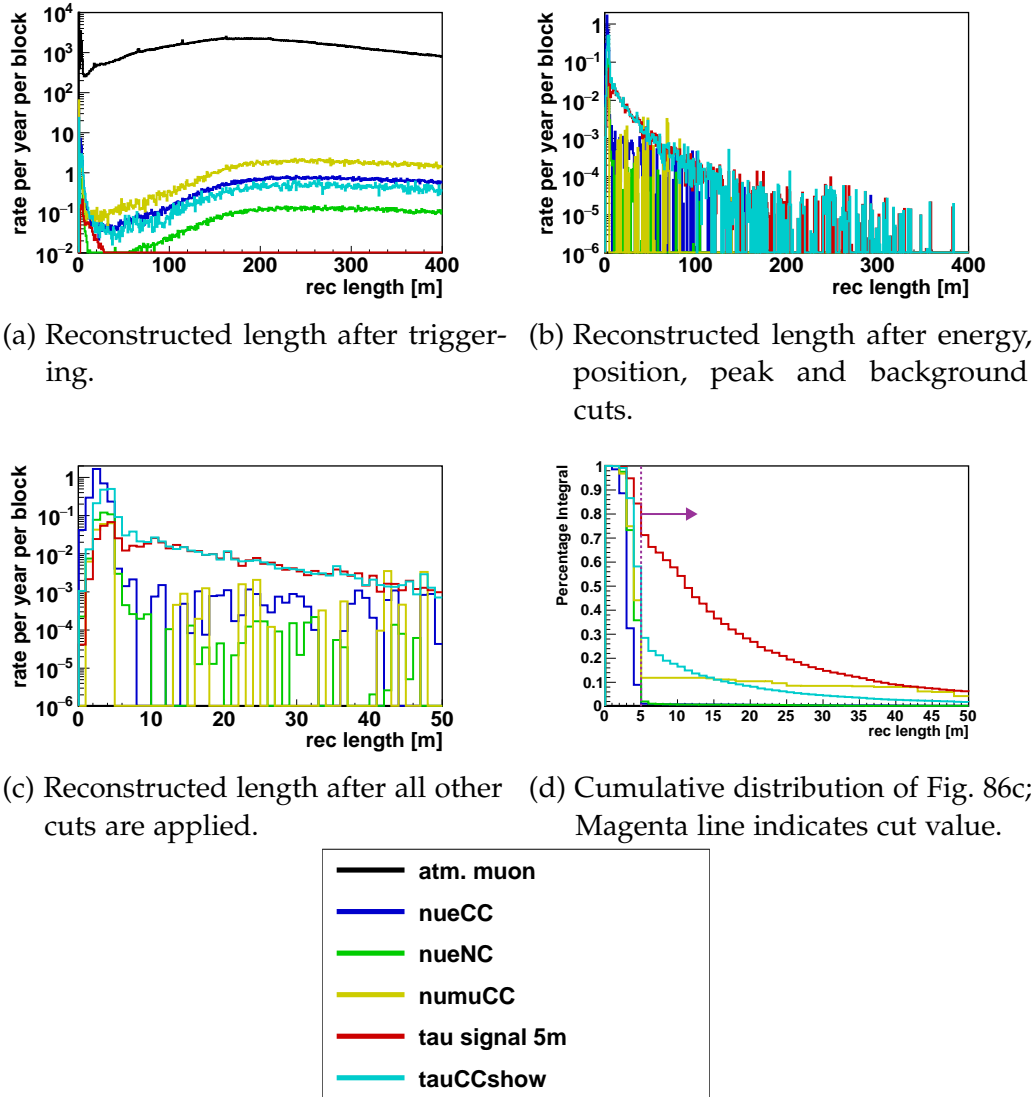|	
——	atm. muon
——	nueCC
——	nueNC
——	numuCC
——	tau signal 5m
——	tauCCshow

Figure 86: Distributions of the reconstructed lengths for the different channels.

events at longer lengths. For the tau signal events the distribution is peaked
at zero with an exponential tail towards longer lengths. The dip at lengths
between 5 m and 7 m is caused by the minimal flight length requirement of
5 m. The events which are wrongly reconstructed typically yield a shorter flight
length than the simulated flight length. Therefore, the dip is only present in the
tau signal and not the tauCCshow distribution.

By selecting events with a reconstructed length larger than 5 m the single
shower and track events are highly suppressed.

6.2 SELECTION CRITERIA EFFICIENCY

The individual efficiencies of the selection criteria give a good indication of their
performance. In order to quantify the performance, two different efficiencies are
calculated for each criterion: the percentage of selected events of all triggered
events (ϵ^{trig}) and the percentage of selected events after applying all other

selection criteria (ϵ^{selec}). The resulting efficiencies are shown in Tab. 2. In the case of ϵ^{selec}, if the other selection criteria rejected all simulated events the efficiency is denoted with "nan". The error estimates for the efficiencies are given in Tab. 8 in the Appendix.

As can be seen from Tab.8, the energy cut applies equally well to all background channels, the background and peak cut mainly reject track like background events, the containment cut rejects atmospheric muons and the length cut rejects single shower events. The efficiencies for the "Double Bang" channels (tau signal and tauCCshow) show some differences for ϵ^{trig} while ϵ^{selec} are comparable. The differences for the ϵ^{trig} are caused by the preselection applied to the tau signal events resulting in a sample of reconstructable "Double Bang" events, whereas the tauCCshow events are dominated by events which are indistinguishable from single shower events. Therefore ϵ^{trig} is significantly lower for all cuts for the tauCCshow events. In the following, the ϵ^{selec} for the tau signal channel is discussed.

The ϵ^{selec} for the tau signal channel shows that the energy cut accepts almost all signal events. This is expected for a successful energy reconstruction, as the requirement for a minimal flight length of 5 m roughly translates to a minimal energy of 100 TeV. The position cut –by construction– reduces the detector volume by around 40 % and therefore rejects the same fraction of the tau signal events. The peak cut rejects around 18 % of the tau signal events. Most of these events have no significant peaks at all. The background cut accepts almost all tau signal events as expected in the case of a successful reconstruction. The length cut rejects around 30 %, these events typically have a large energy inbalance between the two showers (see e.g. in Fig. 55).

The dependence of the efficiencies are evaluated for different Bjorken y and tau flight length values for "Double Bang" events since these are important characteristics (for more details see Chap. 5.1). The selection efficiency given different simulated values for Bjorken y and tau flight length are shown in Fig. 87.

The flight length has a significant impact on the efficiency as shown in Fig. 87a. For flight lengths between 5 m to 10 m the low efficiency of around 0.1 is caused by the reconstruction performance. The efficiency increases and is maximal between 25 m to 50 m. The decrease towards longer lengths is caused by the background cut. At these lengths the finite Prefit direction resolution has a significant impact on the overall performance, causing the background cut to reject signal events. The average efficiency is dominated by small lengths as a result of the steep energy spectrum of the signal.

In principal, it could be assumed that the dependence on Bjorken y is symmetric, as Bjorken y = 0.1 and Bjorken y = 0.9 are two sides of the same coin. This is not the case for two reasons, namely: the vertices always have a fixed relative time ordering, with the neutrino vertex first and the tau decay vertex later, and the tau decay shower on average produces less visible energy than the neutrino interaction. As a result, the efficiency is highest at Bjorken y approaching one and lowest at Bjorken y approaching zero.

Table 2: Selection efficiencies using the selection criteria for the different MC channels; errors are given in Tab. 8.

	energy	position	peak	background	length
			ϵ^{trig}		
atm muon	0.041	0.053	0.003	0.023	0.290
nueCC	0.067	0.183	0.017	0.706	0.849
nueNC	0.047	0.179	0.010	0.705	0.872
numuCC	0.037	0.161	0.003	0.467	0.918
tau signal	0.855	0.417	0.533	0.827	0.698
tauCCshow	0.060	0.183	0.014	0.703	0.864
			ϵ^{selec}		
atm muon	0	0	0	0	nan
nueCC	0.396	0.188	0.168	0.869	0.011
nueNC	0.557	0.222	0.225	0.892	0.020
numuCC	0.349	0.276	0.207	0.061	0.119
tau signal	0.993	0.551	0.816	0.970	0.712
tauCCshow	0.917	0.512	0.684	0.963	0.285
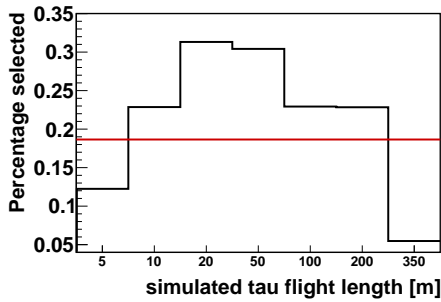
(a) Length.
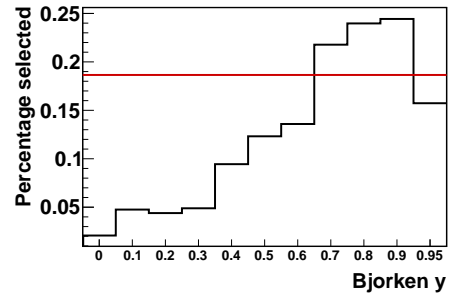
(b) Bjorken y.

Figure 87: Selection efficiency ϵ^{selec} for tauCCshow events for different simulated length and Bjorken y values; red line indicates the average selection efficiency.
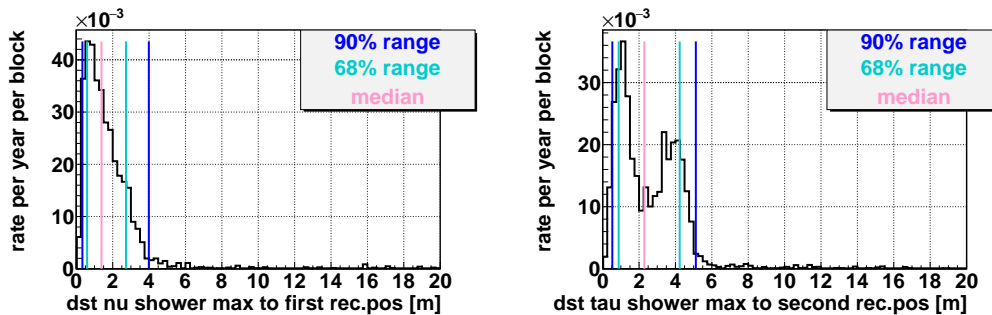
6.3 BELLE STARR RESOLUTION FOR SELECTED EVENTS

In this section the resolutions of the Belle Starr reconstruction chain for "Double Bang" events selected by the final criteria presented. The main focus is on the direction and position reconstruction.

For the position reconstruction the distance between the vertices and the corresponding simulated shower maxima are shown in Fig. 88a and Fig. 88b respectively. Again, the tau decay shower maximum resolution shows the double peak structure due to the difference in shower simulations for charged and neutral pions as discussed in Sec. 5.5.5. Hence, the position resolution is evaluated using the neutrino shower maximum.

A position resolution of 1.5 m median is achieved for the selected events. Compared to the position resolution of 2 m median for all tau signal events as shown in Fig. 77a the position resolution is significantly better. Especially the events in the tail of the distribution are rejected as is indicated by the significant improvement of the 90 % quantiles from 17 m to 4 m. This improvement further supports the selection criteria.

The position resolution results in a tau flight length resolution as shown in Fig. 89. The double peak of the tau shower maximum resolution is smeared by the neutrino shower maximum resolution and is therefore no longer visible. The peak is offset from zero by the difference between simulated flight length and the actual distance between the reconstructed shower maxima (on average 1.5 m). The shower maxima are almost always farther apart due to the energy distribution between the showers and the tau decay shower simulation. In order to give a better impression of the achieved length resolution the reconstructed length for MC events with different simulated length is shown in Fig. 90. As can be seen, for these events the same offset is visible, as they are simulated to have a Bjorken y of 0.9. The achieved length resolution in such a "clean" case is around 1 m FWHM.

The angular resolution is also improved as can be seen from Fig. 91 a median angular resolution of $1.3°$ is achieved compared to the $2°$ for all tau signal

(a) Distance between neutrino shower maximum and first vertex.

(b) Distance between tau shower maximum and second vertex.

Figure 88: Position resolution of the Belle Starr reconstruction chain for tau signal events selected by the final criteria.
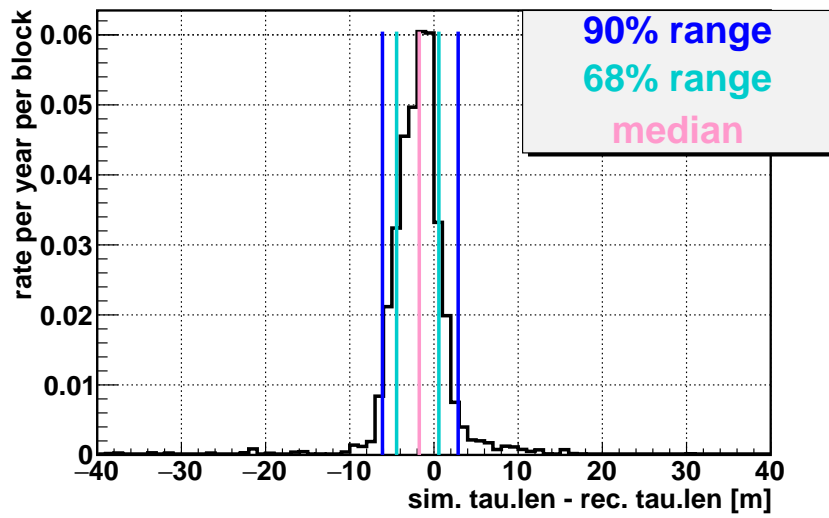
Figure 89: Tau flight length resolution for tau signal events selected by the final criteria.
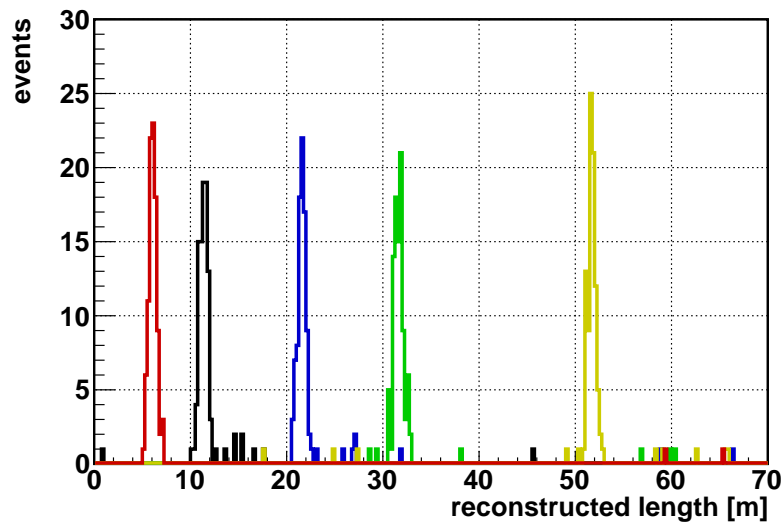

Figure 90: Reconstructed length for Toy MC events with different simulated flight length: 5 m, 10 m, 20 m, 30 m and 50 m from left to right; neutrino energy is 1 PeV and Bjorken y is 0.9 for all events.
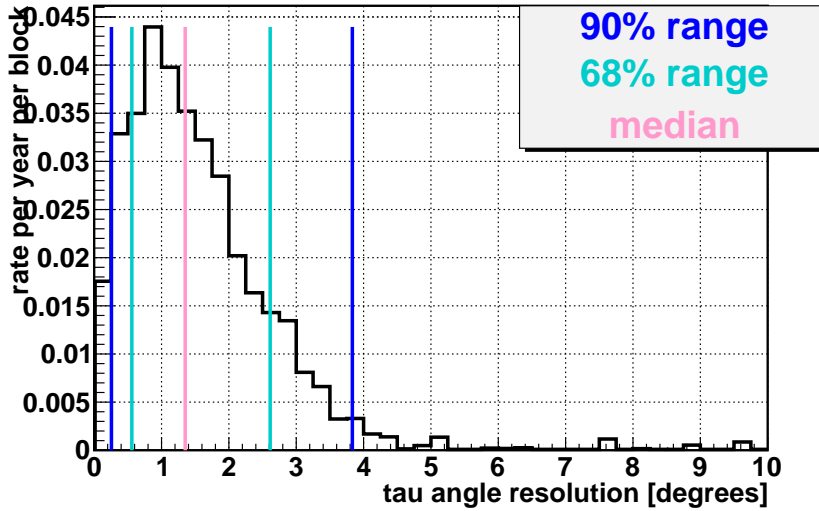
Figure 91: Tau angle resolution for tau signal events selected by the criteria described in Chap. 6.1.

events shown in Fig. 65a. As for the position resolution, the main improvement is achieved by reducing the tails of the distribution as the selection rejects badly reconstructed events and thereby significantly reduces the tails.

The length and direction resolution achieved for the selected events is directly comparable to the performance of AAShowerfit for single shower events as discussed in Chap. 5.3.

6.4 RESULTS OF THE TAU "DOUBLE BANG" SELECTION

The selection of "Double Bang" events presented in this chapter is successful at rejecting other neutrino interaction signatures and atmospheric muon signatures while accepting a significant amount of signal. With all selection cuts applied, the expected rates per year and block are summarized in Tab. 3. The number quoted for the atmospheric muons is an upper limit, as all simulated atmospheric muon events are rejected. The total statistics for atmospheric muons result in a rate per year per block of 0.33. Therefore, this value is quoted. The rates of background neutrino channels are all suppressed to at least one order of magnitude lower than the expected signal rate. The nueNC channel is the only flavor considered for the NC interaction. Since the NC interactions are identical for the three flavors assuming a (1:1:1) flavor ratio the expected total number of NC interactions is three times that of nueNC, i.e. 0.02 per year per block.

The rate of reconstructed "Double Bang" events is sensitive to the assumed neutrino flux. Due to the energy dependence of the tau flight length, the chosen soft spectrum with $\Gamma = 2.46$ and a 3 PeV cut-off is a conservative scenario. A more optimistic scenario is based on a harder spectrum without a cut-off. For example, a harder spectrum of $E^2 \Phi_\nu = 1 \times 10^{-8} (E/\text{GeV}) \, \text{GeV} \, \text{cm}^{-2} \, \text{s}^{-1} \, \text{sr}^{-1}$ per

Table 3: Results of the tau selection for a diffuse neutrino flux with spectral index $\gamma = 2.46$ and a 3 PeV cut-off for one ARCA building block.

channel	rate [per year per block]
atm. muon	0.33
nueCC	0.03
nueNC×3	0.02
numuCC	0.02
tauCCshow	0.48

flavor without a 3 PeV cut-off would result in a signal rate per year per block of 0.55 while keeping the signal to background ratio approximately unchanged.

Since the results depend on the energy, they are expressed as the effective volume and effective area of one building block as a function of the neutrino energy. The effective volume is defined by

$$V_{eff}(E) = V_{gen} \times \frac{N_{selec}(E)}{N_{gen}(E)} \quad , \tag{36}$$

where V_{gen} is the generation volume, $N_{selec}(E)$ is the number of selected events in a given energy range and $N_{gen}(E)$ is the number of generated events in the same energy range. Therefore, the effective volume is the factual volume of the detector in which neutrinos are detected. By dividing the effective volume with the neutrino cross-section the effective area is obtained. The effective area represents the size of a virtual detector which has a 100 % detection efficiency.

The effective volume for a simulated neutrino energy is shown in Fig. 92a. For the numuCC and nueCC channels a spline interpolation is used due to the lack of statistics at high energies. Since the tauCCshow channel is simulated with a smaller spectral index it has sufficient statistics at high energies. For the signal channel, the effective volume is maximal around $\log(E_\nu[GeV]) = 6$. The high energy drop-off corresponds to the lower selection efficiencies at tau flight lengths above 50 m. The drop-off towards lower energies is caused by the energy cut. The numuCC and nueCC channels are approximately flat within the statistical variations. The effective volume for numuCC events has a higher energy threshold since these events deposit only a fraction of the neutrino energy in the detector.

The corresponding effective area are shown in Fig. 92b. It is maximal for the signal towards energies around $\log(E_\nu[GeV]) = 6.5$. This difference between effective volume and area is caused by the neutrino cross-section which monotonously increases with energy. Therefore, events at the highest energies corresponds to a large effective area.
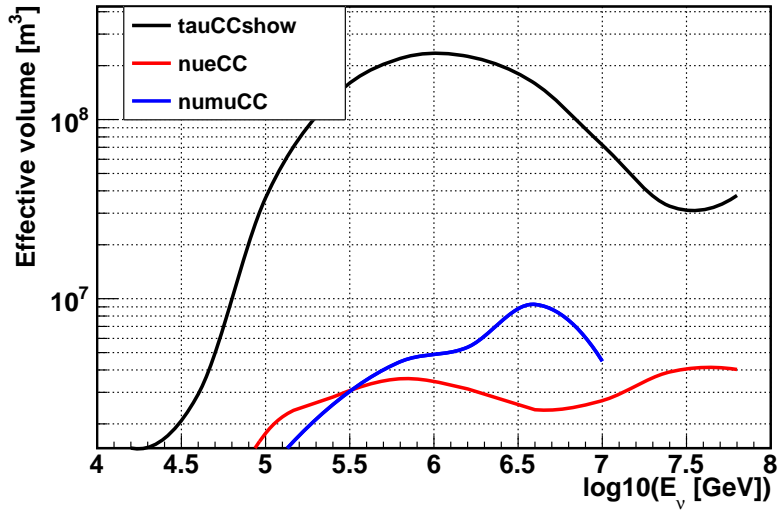
(a) Effective volume after selection cuts.
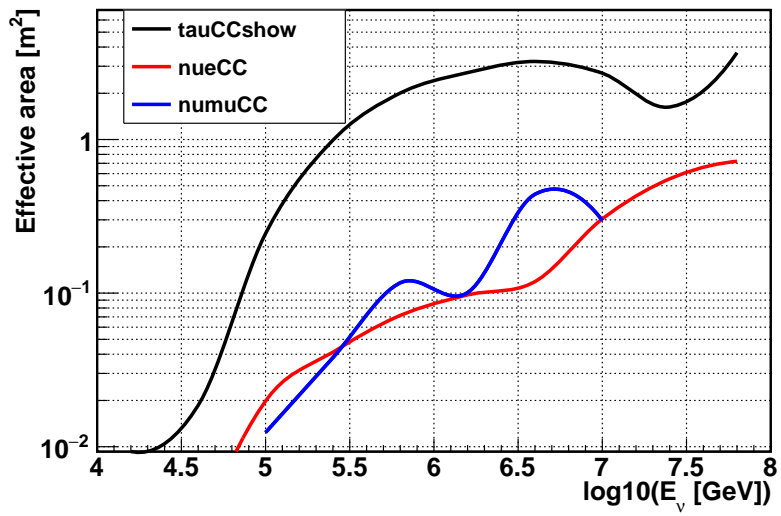
(b) Effective area after selection cuts.

Figure 92: Studies of the effective area and volume for one ARCA building block for a spectral index of $\Gamma = 2.46$ and a 3 PeV cut-off.

6.5 DISCUSSION

The direct detection of "Double Bang" events using the KM3NeT/ARCA detector touches on multiple topics of current scientific research. On the one hand, observed tau events can contribute significantly to the identification and characterization of an astrophysical neutrino flux. On the other hand, direct observations of tau neutrino interactions have only been performed by two experiments so far and in a completely different energy regime.

The tau neutrino events relate more directly to an astrophysical signal than electron or muon neutrinos for two reasons. Firstly, the background from atmospheric tau neutrinos is expected to be negligible so that tau events in principle yield a larger significance than electron or muon events. Secondly, the tau identification greatly benefits a flavor composition analysis since without tau identification a degeneracy in the flavor composition remains.

In order to evaluate the performance of Belle Starr, the results are compared to the results of the IceCube collaboration for a tau identification algorithm [122]. The IceCube algorithm identifies tau events by looking for a double pulse structure in the signal recorded by the PMTs. Therefore, only a "Double Bang" identification and no reconstruction of the two vertices is performed. This so-called "Double Pulse" algorithm achieves a tau identification of 0.22 events per year at a total expected background rate of 0.1 for all cosmic neutrino background channels for an assumed neutrino flux of $E^2\Phi_\nu = 1 \times 10^{-8} \, (E/GeV) \, GeV \, cm^{-2} \, s^{-1} \, sr^{-1}$ per flavor.

In comparison, the Belle Starr algorithm identifies 0.55 tau events per year per ARCA block at a total expected background rate of 0.09 for all cosmic neutrino background channels. Additionally, the Belle Starr algorithm reconstructs the position of the two showers while the Double Pulse algorithm only identifies tau events. Considering, that a single ARCA block is around 2/3 the instrumented volume of the IceCube detector, the Belle Starr algorithm clearly performs better than the Double Pulse algorithm.

This better performance is due to three main factors: the multi-PMT design of KM3NeT, the detection medium and the two shower position reconstruction. The multi-PMT design offers excellent atmospheric muon rejection. The detection medium of KM3NeT is liquid water and that of IceCube is ice. In water, light suffers less from scattering and therefore a better timing resolution is achieved. In ice, optical backgrounds are greatly reduced, but due to the KM3NeT multi-PMT design the influence of these backgrounds are small. Last but not least, the two shower position reconstruction significantly improves the background rejection by allowing for powerful selection criteria.

The direct detection of tau neutrinos has been achieved by two experiments so far, namely: DONUT and OPERA. Both experiment observed tau neutrinos using a nuclear emulsion technique. In order to achieve the required tau tagging these detectors are designed to detect tau neutrino interactions at tau flight lengths in the $\mathcal{O}(mm)$ range. The final analysis of the DONUT experiment [123] yielded 9 tau candidates in 5 months of data taking. The OPERA experiment

found a total of 5 tau events in 4 years of observation. Resulting in a 5σ discovery on $\nu_\mu \to \nu_\tau$ appearance [124].

Compared to these precision experiments, the Belle Starr reconstruction for KM3NeT/ARCA adds a possibility to observe tau neutrinos from the cosmos at unprecedented energies. With the full realization of KM3NeT consisting of 6 ARCA blocks, the largest sample of tau neutrino interactions in the world could be recorded.